(2)

TGAL-92-13

Land-based Seismic Array Studies of Low Frequency Ambient Oceanic Noise

Robert K. Cessaro

Teledyne Geotech Alexandria Laboratories
314 Montgomery Street
Alexandria, Virginia 22314-1581

FEBRUARY 1992

FINAL TECHNICAL REPORT

PROJECT TITLE: Land-based Seismic Array Studies of Low Frequency Ambient Oceanic Noise

CONTRACT: N00014-90-C-0118

Approved for publication and release. Submitted to *Bulletin of the Seismological Society* (paper I) and *Geophysical Research Letters* (paper II).

Prepared for:
Office of Naval Research
Code 1125GG
800 N. Quincy St.
Arlington, VA 2217-5000

Paper I

Sources of Primary and Secondary Microseisms

by
Robert K. Cessaro
Teledyne Geotech Alexandria Laboratories
314 Montgomery Street
Alexandria, VA 22314

Submitted to:
Bulletin of the Seismological Society of America

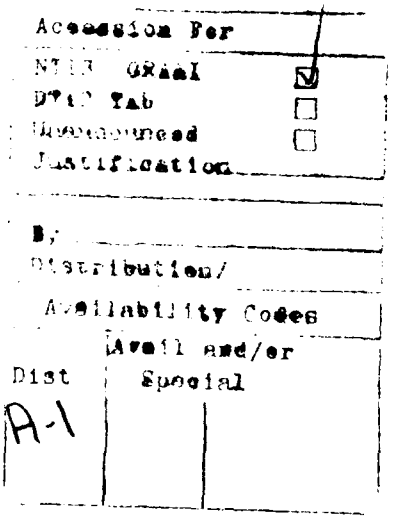

Sources of Primary and Secondary Microseisms

ROBERT K. CESSARO

Teledyne Geotech Alexandria Laboratories, Alexandria, Virginia

For submission to BSSA

ABSTRACT

Low frequency (0.01 to 0.2 Hz) seismic noise, arising from pelagic storms, is commonly observed as microseisms in seismic records from land and ocean bottom detectors. One principal research objective, in the study of microseisms, has been to locate their sources. This paper reports on an analysis of primary and secondary microseisms recorded simultaneously on three land-based long-period arrays (Alaskan Long Period Array, Montana Large Aperture Seismic Array, and Norwegian Seismic Array) during the early 1970's. Reliable microseism source locations are determined by wide-angle triangulation, using the azimuths of approach obtained from frequency wave-number analysis of the records of microseisms propagating across these arrays. Two near-shore sources of both primary and secondary microseisms appear to be persistent in the sense that they are associated with essentially constant near-shore locations. Secondary microseisms are observed to emanate from wide ranging pelagic locations in addition to the same near-shore locations determined for the primary microseisms.

INTRODUCTION

Microseisms, the persistent oscillations of seismic waves unrelated to earthquakes, explosions or local noise sources, have been observed on seismic records since the 19th century (Bertelli, 1872). Since then, locating their source has been a fundamental research goal in their study. Studies early in this century proposed their association with meteorological storm systems in the ocean. More recently, numerous observations have been made both on land and on the ocean bottom. Microseisms are characterized by long period waves with dominant periods between 2 and 40 seconds. These waves have been interpreted as short-period P waves, higher mode surface waves, long period surface waves, and ultra-long period surface waves. Microseisms propagating as long period surface waves were identified by Haubrich *et al.* (1963) as primary- and double-frequency (or secondary) microseisms, covering two distinctly different frequency bands: 80 mHz and 150 mHz, respectively. The association of primary and secondary microseisms with the same atmospheric disturbance was first noted by by Oliver and Page, (1963) who also observed that primary microseisms have twice the dominant periods of the related secondary microseisms. Several mechanisms for the generation of these two types of microseisms have been postulated in recent work.

Primary microseisms are observed on land between about 40 and 80 mHz (e.g., Oliver, 1962; Oliver and Page, 1963; Haubrich *et al.*, 1963; Haubrich and McCamy, 1969; Darbyshire and Okeke, 1969). Their spectral peak reflects the wavelengths of the dominant

ocean waves and appear to form in shallow water by the interaction of ocean swells with a shoaling ocean bottom (*Oliver*, 1962; Haubrich *et al.*, 1963).

Secondary or double-frequency microseisms are commonly observed, with dominant peak frequencies between 100-160 mHz or approximately double that of the peak ocean wave frequencies. They are observed on land (e.g., *Bernard* 1941; *Iyer*, 1958; *Darbyshire*, 1950; *Hasselmann*, 1963, *Haubrich*, 1963) and may be generated in either shallow or deep water. An early theoretical work by Miche (1944) suggested that low-frequency sea-bottom pressure perturbations could be generated by the nonlinear interaction of surface ocean waves. Expanding on Miche's work, Longuet-Higgins (1952) proposed that double-frequency microseisms arise from nonlinear second-order pressure perturbations on the ocean bottom caused by the interference of two ocean waves of equal wavelengths traveling in opposite directions. In a study of double-frequency microseisms recorded at LASA, *Haubrich and McCamy* (1969) concluded that they result primarily from coastal reflection of ocean waves.

Several studies have shown that the ocean-bottom microseism spectrum is similar in shape to the continental microseismic spectrum but with greater amplitude and correlate well with known storm systems (Bradner and Dodds, 1964; Bradner *et al.* 1965, 1970; Latham and Sutton, 1966); Latham and Nowroozi, 1968). Analysis of OBS data recorded near a cyclonic source suggests that microseisms arise from non-linear interaction of storm waves (Ostrovsky and Rykunov, 1982). Deep-ocean pressure and electric field measurements show that pressure signals are correlated with the changing wind field ac-

companying storm passage and associated low-frequency acoustic waves generated in the atmosphere (Webb and Cox, 1986).

Most recent studies of microseisms have attempted to determine the directions of approach, phase velocity, the location of the source, and in some cases, to study structural and sediment properties (Darbyshire, 1954; Iyer, 1958; Toksöz, 1964; Latham and Nowroozi, 1968 Bossolasco *et al.*, 1973; Asten and Henstridge, 1984; Yamamoto and Torii, 1986). Microseisms appear to propagate mainly by Rayleigh wave motion but may contain Love wave components where propagation is through uninterrupted layered structure (Rind and Donn, 1979).

Analysis of low-frequency land-recorded seismic array data has provided a better understanding of the nature of the low frequency noise (seismic and acoustic) generated by large pelagic storms that propagates into the continental interior as microseismic surface waves. Haubrich and McCamy (1969) and Toksöz and Lacoss (1968) studied frequency-wave number spectra of microseism recordings at the Large Aperture Seismic Array (LASA) to detail microseismic sources and propagation modes. Capon (1972), suggested the coincidence of an atmospheric low pressure region with a microseism source determined from simultaneous frequency-wavenumber analysis of LASA and ALPA long-period data. Other studies using small array data have been used to examine microseismic surface wave sources (e.g., Szelwis, 1980, 1982). From analysis of a three-day sample of primary microseisms obtained from two large aperture arrays, Cessaro and Chan (1989)

found two near-shore source locations that were associated with nearly all of the coherent primary microseisms propagating across two arrays.

This paper reports on the progress of research begun in 1988 (Cessaro and Chan, 1989). The current study extends the analysis to secondary microseisms with a larger sample of microseisms, and it includes the redundancy afforded by one additional array. The expanded observations of primary microseisms have provided confirmation of the preliminary results showing two persistent near-shore sources of primary microseism noise that are clearly associated with pelagic storm systems but not as a close function of their locations (Cessaro and Chan, 1989). In addition, secondary microseism sources are also observed from the same two persistent northern hemisphere near-shore locations but are also observed to emanate from other ephemeral pelagic sources more closely related to storm locations.

DATA DESCRIPTION

The low-frequency microseism signals are obtained from digitized recordings collected by the Montana Large Aperture Seismic Array (LASA), Alaskan Long Period Array (ALPA), and Norwegian Seismic Array (NORSAR) for the period 00:00 UTC 25 Nov 1973 and to 00:00 UTC 29 Nov 1973. The LASA array, operating from 1965 through 1978, included 21 three-component long-period seismometers. The ALPA array, operating from 1970 through 1982, was composed of 19 long-period triaxial seismometers. The NORSAR array included 22 long-period seismometers during the operating period 1971 to 1976.

The arrays recorded digitally at 1-Hz sampling frequency. The frequency response of the long-period elements of the arrays is flat to velocity from 25- to 200-second period (5-40 mHz). The location and pattern of each array are shown in Figure 1. The differences in array dimensions and geometries are reflected in the resolution observed in the FK analysis of their respective data.

Continuous 4000-second data samples are excerpted for analysis on an interval of approximately 6-hours from the long-period array data archive (Teledyne Geotech Alexandria Laboratories). Signals are taken from vertical-component channels for LASA and NORSAR and mathematically-rotated vertical component channels for ALPA. Signals are bandpass filtered using 4-pole Butterworth filters centered at 16-sec (0.06 Hz) and 8-sec (0.12 Hz). No attempt is made to correct for instrument response (nominally 25 sec), since it has proved unnecessary for FK analysis.

Some of the data samples are shifted by as much as an hour from the regular 6-hour interval in order to avoid large earthquake phases exhibiting substantial power in the same pass bands. These earthquake phases are confirmed on the ISC Bulletin reporting origin times and hypocenters. Although these phases are not directly useful to the objective of this study, they do provide an indirect means of calibrating the accuracy of the microseism approach azimuths obtained from the FK analysis. Earthquake phases, examined in the microseism frequency bands, give approach azimuths that are typically within one degree of the theoretical azimuth over the range of azimuths encountered for the microseisms.

ANALYSIS

Frequency-wavenumber analysis

Frequency wavenumber (FK) analysis is performed on samples of low-frequency ambient noise recorded during the activity of a series three pelagic storm systems to determine dominant phase velocities and approach azimuths. The ambient noise field recorded during the study period consists of both coherent and incoherent components. The incoherent component, primarily from sources near the array, does not appear as separable power peaks in the F-K analysis. The coherent component consists of microseisms from multiple sources and earthquakes. The sampled time periods are selected by searching the Mariner Weather Log (1973) log covering the northern hemisphere peak storm months for the presence of isolated principal cyclone tracks occurring simultaneously in the North Atlantic and the North Pacific oceans while the three seismic arrays were in full operation.

Microseisms arriving as surface waves from pelagic storms are examined for temporal and spatial variation in phase velocity and direction of approach by using a sliding-window, broad-band FK technique (Capon, 1969) on 4000-sec bandpassed digitized array data samples. The term 'FK' analysis is used here as a convenience; it is more accurately referred to as frequency-slowness analysis, because the frequency-wave-number power spectrum are examined for specific band-limited frequency planes. FK analysis is performed on sequential 128-second data segments in the 4000-sec data sample. Signal time

windows are advanced by 100 seconds from previous windows, resulting in adjacent window overlaps of 28 seconds. Resulting estimates of approach azimuth and phase velocity are collected and examined for consistency and distribution. Figure 2 shows an example of the results of FK processing. The contours shown represent 1 dB increments in power referred to the window maximum for a frequency given band. Multiple FK power peaks obtained from each 4000-sec data sample provide many approach azimuths that contribute to the suite of potential microseismic source locations. Since the microseisms are observed to propagate in the form of Rayleigh waves, the approach azimuths used are limited to those attended by phase velocity observations between 3.0 and 4.0 km/sec (*e.g.*, Capon, 1970). Time windows containing low-frequency phases from known earthquakes are excluded from this analysis.

Spectral analysis

Averaged spectra obtained for signals from one vertical-component in each array show that power in the two microseism bands correlate well with storm intensity (e.g., *Korhonen and Pirhonen*, 1976). The variations in spectral power and peak frequencies are consistent with the storm intensities reported in the Mariners Weather Log (1973). An order of magnitude fluctuation in both the primary and secondary microseism amplitudes are typically observed over a time scale of minutes during the passage of these storms.

The spectra observed in each array record represent a composite of distant and local sources. Incoherent local spectral components are reduced as the spectra are averaged.

Spectral components from the activity of distant storms occurring simultaneously in the Atlantic and Pacific ocean are enhanced by averaging, particularly if they can be separated by beam forming. The time histories of primary microseism spectra, observed over a time period where two storms are active, can be separated by noting the primary microseism spectra and associated dominant FK power peaks for the same data window. The separation of spectral components is improved by beam forming on the azimuth associated with one of the dominant FK peaks at a time when the other peak is temporarily weak or absent (Figure 3). In general, microseisms arising from the action of several storms exhibit different spectral characteristics and histories that can be followed separately in the time-history of their respective power spectra. It can be adduced from this analysis that the approach azimuths determined for these data samples are from the microseisms evident in the time-series record rather than from any localized source.

Obtaining microseism source locations by triangulation

A wide aperture triangulation is performed on simultaneous approach azimuth observations made from ALPA, LASA and NORSAR array data by combining the estimates of approach azimuths obtained from the FK analysis over each 4000-sec data sample. This approach represents an improvement in resolution of distance and azimuth between sources and receivers compared with that obtained from earlier array studies (Toksöz and Lacoss, 1968; Lacoss, *et al.*, 1969; Capon, 1969, 1970, 1972). Most earlier array studies did not attempt to triangulate and so provided only limited information on distance from source to receiver. The estimates of azimuth and velocity stability and associated errors

are obtained from the distribution of approach azimuths, velocity and their corresponding FK power. In this way, each 4000-sec data sample provides several representative approach azimuths along with corresponding estimates of their reliability. Figure 4 shows a typical distribution of primary microseism approach azimuths determined for the time windows used within a single 4000-point data sample. The intersection of separate map projections of these azimuths and error estimates from their respective arrays provide bounding estimates of the microseism source location. Estimates from three arrays is most useful, since it provides some redundancy in the technique.

RESULTS AND DISCUSSION

Both primary and secondary microseism spectral power is observed to vary by more than an order of magnitude over a time scale of minutes. Modulation of their corresponding FK power peaks is qualitatively consistent with the spectral power variations. The existence of multiple storms during the sampled data times is reflected in the peak frequencies observed, i.e., microseisms from each storm exhibited distinctive peak frequency histories as their surface winds developed, moved and dissipated. The sliding window technique applied to FK analysis has provided temporal and spatial information about the microseism sources, factors particularly important for characterizing secondary microseisms.

FK analysis may be regarded as a measure of microseismic wave field coherency, in the sense that it detects the coherent fraction of the total storm-related microseismic noise

field. Primary microseisms appear to arise from deterministic spatially limited sources while secondary microseism locations suggest sources that are both deterministic and stochastic.

Primary microseism sources

Wide angle triangulation using approach azimuths obtained by these methods confirms the results of preliminary work (Cessaro and Chan, 1988) and shows that primary microseisms emanate from persistent near-shore locations that do not correlated well with their associated pelagic storm locations. During the time period sampled for this study, three major storms were active in the North Pacific and Atlantic oceans and two primary microseism source locations are identified: (1) A wide ranging North Pacific storm correlates with a microseism source near the west coast of the Queen Charlotte Islands, BC and (2) Two North Atlantic storms correlate well with a source near the coast of Newfoundland (Figure 5). While the North Pacific storm trajectory subtends an arc greater than 90° from the LASA array, the associated primary microseism source appears to be stable (Figure 5). The microseism source near Newfoundland exhibits similar stability.

Secondary microseism sources

In addition to the same near-coastal source locations observed for primary microseisms, meandering (time-variant) oceanic sources are also observed for secondary microseisms arriving from north Pacific and north Atlantic storms. The oceanic source is more close-

ly associated with the storm trajectory, in the sense that the locations remain within the synoptic area of the storm path. For example, a storm path in the western North Atlantic is attended by secondary microseism sources that also appear to be in that region. The oceanic locations of time-variant secondary microseism are made more difficult by the uncertainty in the triangulation position imposed by the differences in microseism source-to-receiver travel times for the possible combinations of source and arrays positions. Once a trial triangulation position is determined, the differences in travel times to the arrays is considered and the appropriate data windows and their respective approach azimuths are examined to insure that the trial location is consistent. This problem does not arise for the time-invariant near-coastal microseism source. The positions shown in Figure 6 are obtained by triangulation considering travel time differences.

CONCLUSION

Although pelagic storms provide the source of microseismic wave energy, it is the interplay between (1) the pelagic storm parameters, such as tracking velocity, peak wind speed, location, effective area, and ocean surface pressure variation, (2) the resulting storm waves and their wave number distribution, (3) the direction of storm wave propagation, and (4) the near-shore and deep-ocean processes that control the production of microseisms. It is apparent that only a fraction of the total storm-related noise field is coherent. From the perspective of a seismic array, at any given moment only the most energetic coherent portion of the noise field is detected by FK analysis, *i.e.*, a peak in the FK power represents the most energetic coherent portion of the microseismic wave field

at that instant. FK analysis is sensitive, therefore, to only a small part of the total noise field. It is also shown that both the primary- and secondary-microseism source locations do not appear to follow the storm trajectories directly. Secondary microseism source locations exhibit a duality in the sense that one is shared by the primary microseism source while the other meanders within the synoptic region of peak storm wave activity. With the several storms analyzed so far, it appears that the observed relationships between the changing storm parameters and resulting shifts in secondary microseisms locations are typical. It is not known why particular near-shore locations radiate strong coherent primary and secondary microseisms. It may be a combination of local resonance modes and storm wave approach and reflection interactions. There appear to be at least two specific near-shore regions in the northern hemisphere that generate microseisms strong enough to be observed as persistent FK power peaks in both the secondary- and primary-microseism bands regardless of the storm location within the associated North Atlantic or Pacific ocean basin, provided the storm-generated surface water waves are sufficiently energetic. Preliminary analysis of microseisms recorded during the peak storm periods for the southern hemisphere suggests the existence of persistent sources there also (Cessaro, 1991).

REFERENCES

Asten, M. W. and J. D. Henstridge (1984). Array estimators and the use of microseisms for reconnaissance of sedimentary basins, *Geophysics*, **49**, 1828-1837.

Bernard, P. (1941). Sur certaines proprietes de la houle etudiees a l'aide des enregistrements seismographiques, *Bull. Inst. Oceanogr. Monaco*, **800**, 1-19.

Bertelli, T. (1872). Osservazoni sui piccoli movimenti dei pendoli in relazione ad alucuni fenomeni meteorologiche, *Boll. Meteorol. Osserv. Coll. Roma*, **9**, 10 pp.

Bossolasco, M., G. Cicconi, and C. Eva (1973). On microseisms recorded near a coast, *Pure Appl. Geophys.*, **103**, 332-346.

Bradner, H. and J. G. Dodds (1964). Comparative seismic noise on the ocean bottom and on land, *J. Geophys. Res.*, **69**, 4339-4348.

Bradner, H., J. G. Dodds, and R.E. Foulks (1965). Investigation of microseism sources with ocean-bottom seismometers, *Geophysics*, **30**, 511-526.

Bradner, H., L. de Jerphanion, and R. Langlois (1970). Ocean microseism measurements with a neutral buoyancy free-floating midwater seismometer, *Bull. Seism. Soc. Am.*, **60**, 1139-1150.

Capon, J. (1969). High resolution frequency-wavenumber spectrum analysis, *Proc. IEEE*, **57**, 1408-1418.

Capon, J. (1970). Analysis of Rayleigh-wave multipath propagation at LASA, *Bull. Seism. Soc. Am.*, **60**, 1701-1731.

Capon, J. (1972). Long-period signal processing results for LASA, NORSAR and ALPA, *J. R. astr. Soc.*, **31**, 279-296.

Cessaro, R. K. (1991). Seismic Array Study of Primary and Secondary Microseisms, *EOS, Trans. Am. Geophs. Un.*, **72**, 302-303.

Cessaro, R. K. and W. W. Chan (1989). Wide-angle triangulation array study of simultaneous primary microseism sources. *J. Geophys. Res.*, **94**:15,555-15,563.

Darbyshire, J. (1950). Identification of microseismic activity with sea waves, *Proc. R. Soc. Lond. Ser. A*, **202**, 439-448.

Darbyshire, J. (1954). Structure of microseismic waves: Estimation of direction of approach by comparison of vertical and horizontal components, *Proc. R. Soc. Lond. Ser. A*, **223**, 96-111.

Darbyshire, J. and E. O. Okeke (1969). A study of primary and secondary microseisms recorded in Anglesey, *Geophys. J. R. astr. Soc.*, **17**, 63-92.

Hasselmann, K. (1963). A statistical analysis of the generation of microseisms, *Rev. Geophys. Space Phys.*, **1**, 177-210.

Haubrich, R.A. and K. McCamy (1969). Microseisms: coastal and pelagic sources, *Rev. Geophys. Space Phys.*, **7**, 539-571.

Haubrich, R. A., Munk, W. H. and F. E. Snodgrass (1963). Comparative spectra of microseisms and swell, *Bull. Seism. Soc. Am.*, **53**, 27-37.

Iyer, H. M. (1958). A study of direction of arrival of microseisms at Kew Observatory, *Geophys. J.*, **1**, 32-43.

Latham, G. V. and A. A. Nowroozi (1968). Waves, weather, and ocean bottom microseisms, *J. Geophys. Res.*, **73**, 3945-3956.

Latham, G. V. and G. H. Sutton (1966). Seismic measurements on the ocean floor, 1. Bermuda Area, *J. Geophys. Res.*, **71**, 2545-2573.

Longuet-Higgins, M. S. (1950). A theory of the origin of microseisms, *Phil. Trans. Roy. Soc. London*, **243**, 1-35.

Miche, M. (1944). Mouvements ondulatoires de la mer en profondeur constante ou decroissante, *Annales des Ponts et Chaussees* 114, 25-78.

Mariners Weather Log, U. S. Dept. of Commerce, NOAA, Natl. Environ. Satellite, Data and Information Service (U. S. Govt. Print. Office), Washington, D.C., 1970-1973.

Oliver, J. (1962). A worldwide storm of microseisms with periods of about 27 seconds, *Bull. Seism. Soc. Am.*, **52**, 507-517.

Oliver, J. and R. Page (1963). Concurrent storms of long and ultra-long period microseisms, *Bull. Seism. Soc. Am.*, **53**, 15-26.

Ostrovsky, A. A. and L. N. Rykunov (1982). Experimental study of ocean bottom seismic noise during passage of a cyclone, *Oceanology*, **22**, 720-722.

Rind, D. and W. Donn (1979). Microseisms at Palisades, 2, Rayleigh wave and Love wave characteristics and the geologic control of propagation, *J. Geophys. Res.*, **84**, 5632-5642.

Sorrells, G. G., McDonald, J. A., Der, Z. A. and E. Herrin (1970). Earth motion caused by local atmospheric pressure changes, *Geophys. J. R. astr. Soc.*, **26**, 83-98.

Szelwis, R. (1980). Inversion of microseismic array cross spectra, *Bull. Seism. Soc. Am.*, **70**, 127-148.

Szelwis, R. (1982). Modeling of microseismic surface wave sources, *J. Geophys. Res.*, **87**, 6906-6918.

Toksöz, M. N. (1964). Microseisms and an attempted application to exploration, *Geophysics*, **29**, 154-177.

Toksöz, M. N. and R. T. Lacoss, (1968). Microseisms: mode structure and sources, *Science*, **159**, 872-873

Webb, S. C., and C. S. Cox (1986). Observations and modeling of seafloor microseisms, J. Geophys. Res., 91, 7343-7358.

Wiechert, E. (1904). *Verhandlungen der Zweiten Internationalen Seismologischen Konferenz. Gerl. Beitr. Geophys.*, Erganzungsbd. 2, 41-43.

Yamamoto, T., and T. Torii (1986). Seabed shear modulus profile inversion using surface gravity (water) wave-induced bottom motion, Geophys. J. R. astr. Soc., 85, 413-431.

FIGURES

Figure 1. The location and patterns of LASA, NORSAR and ALPA seismic arrays (drawn to the same scale).

Figure 2. Example of the results of FK processing for single frequency microseism signals recorded on the NORSAR array. The contours shown represent 2 dB increments in power referred to the window maximum for the 0.04 - 0.08 Hz frequency band. The coordinates are in units of slowness in x and y.

Figure 3. Example of the microseism spectra improved by beam forming on azimuths associated with each of the dominant primary microseism FK peaks at a time when the other peak is temporarily weak or absent. The power is shown in dB relative to an arbitrary reference and the spectra are uncorrected for instrument response.

Figure 4. Example of the binned distribution of primary microseism approach azimuths determined with data for time windows used during the period Nov. 25-29, 1973 for NORSAR array; (a) Power weighted FK peaks by azimuth and time (5° azimuth bin), (b) Power weighted FK peaks by azimuth and velocity (5° azimuth, 0.25 km/sec velocity bins).

Figure 5. Maps showing the two persistent primary microseism source locations determined by wide angle triangulation of approach azimuths. Projection widths are drawn from the half power bounds in the approach azimuth distribution. (a) North Pacific storms are associated with a microseism source near the west coast of the Queen Charlotte Islands, (b) North Atlantic storms generate result in sources located near the coast of Newfoundland.

Figure 6. Map showing the positions of secondary microseism sources for storms in the north Pacific and Atlantic oceans, obtained by triangulation considering travel time differences. Position boundaries are drawn from the projection of half power limits in the approach azimuth distribution determined for data from each array. The numbers refer to the sample sequence number for an interval spacing of 6 hours over the period Nov. 25-29, 1973.

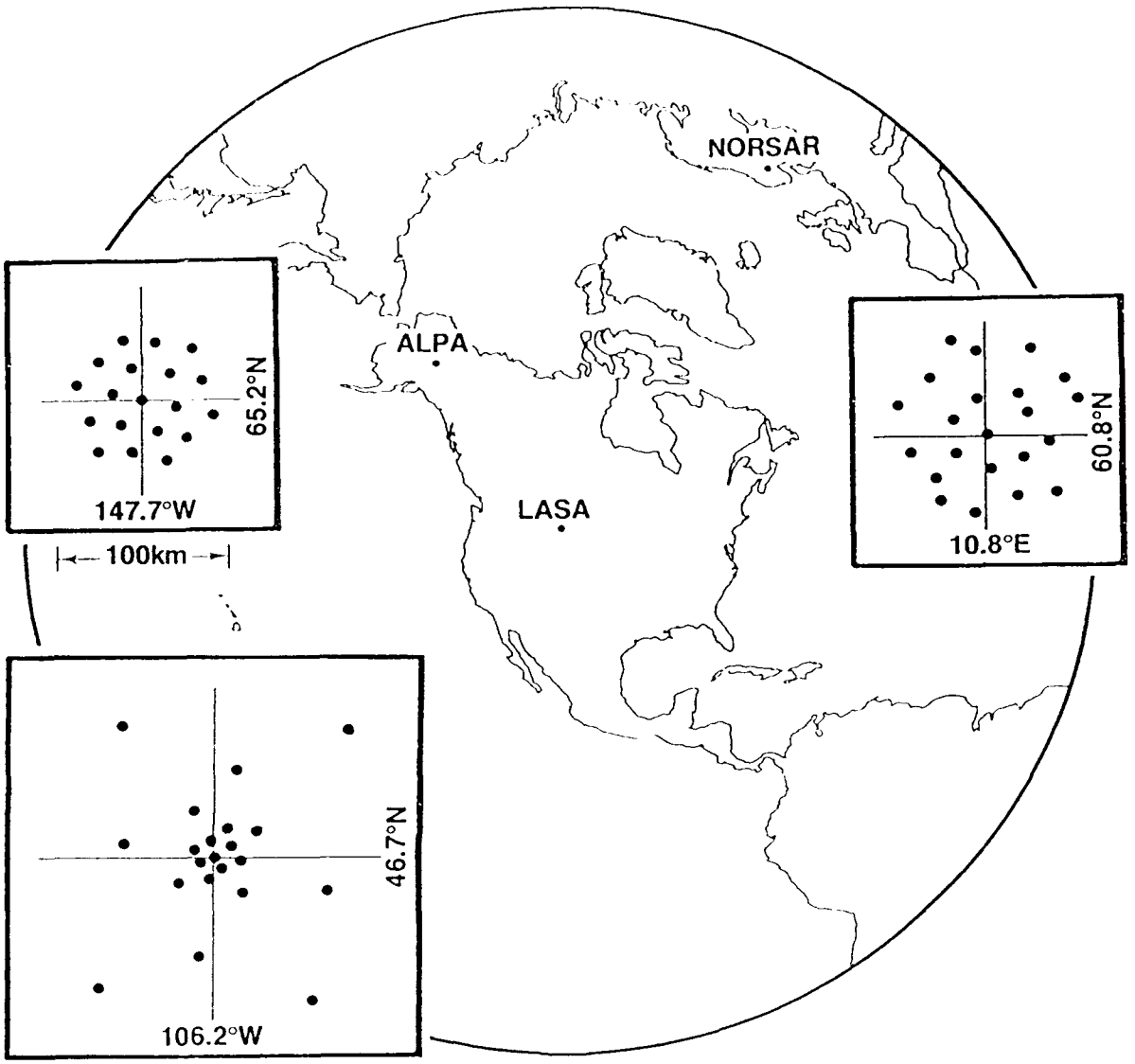

FIGURE 1.

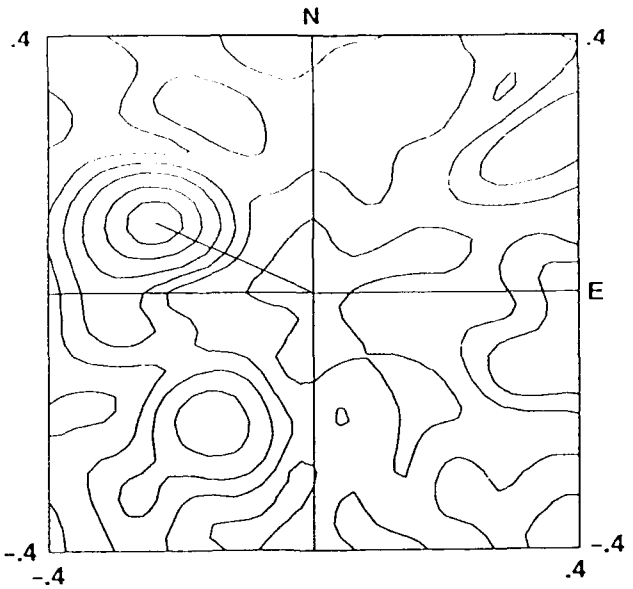

FIGURE 2.

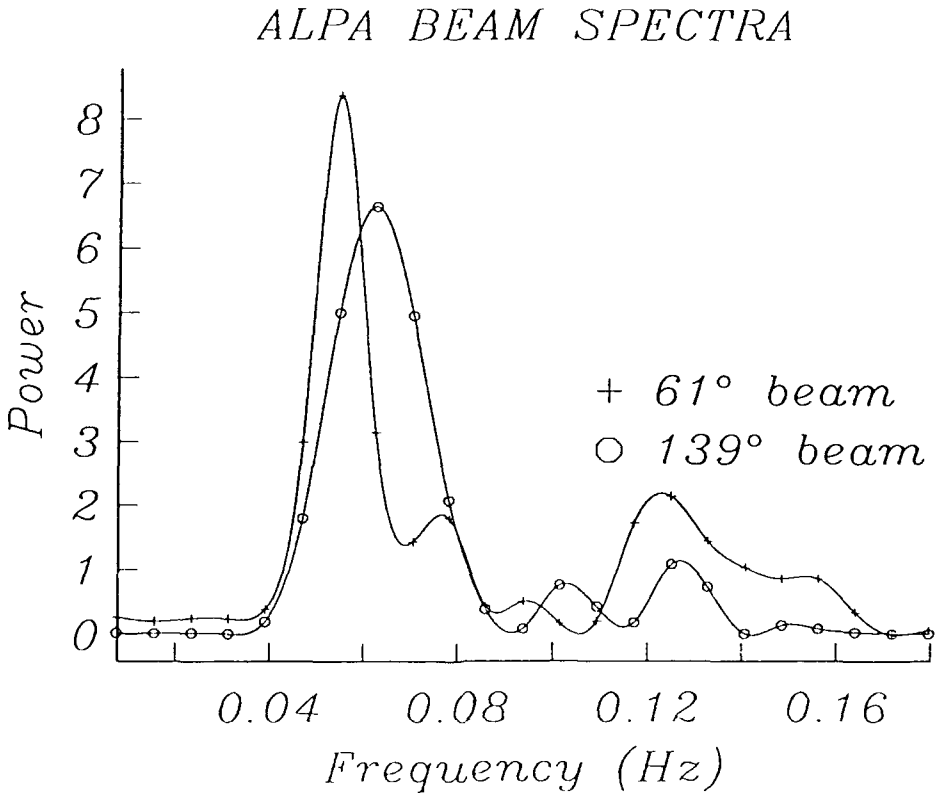
ALPA BEAM SPECTRA
Power
8
7
6
5
4
3
2
1
0
+ 61° beam
○ 139° beam
0.04
0.08
0.12
0.16
Frequency (Hz)

FIGURE 3.

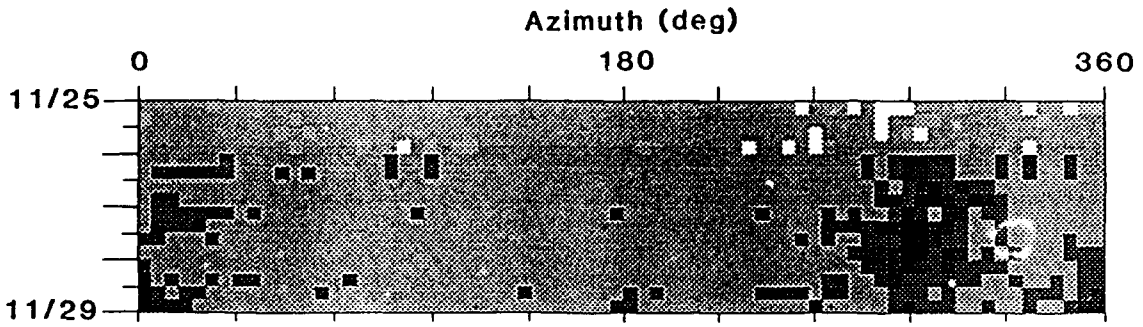

FIGURE 4a.

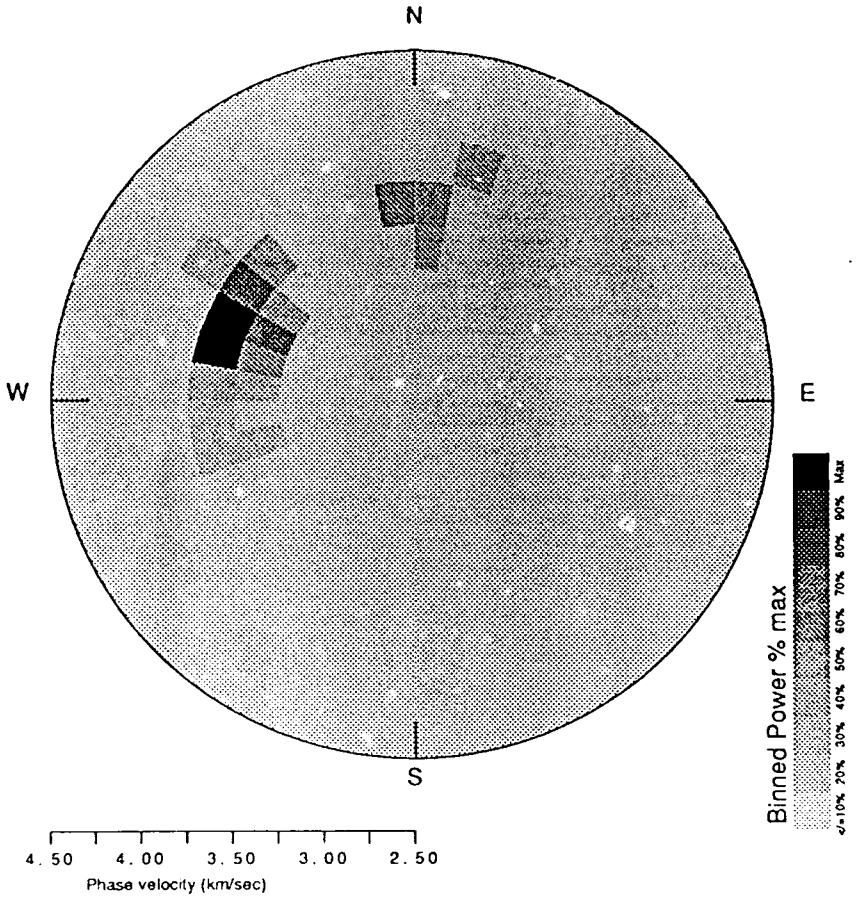
N
W
E
S
Binned Power % max
<10% 20% 30% 40% 50% 60% 70% 80% 90% Max
4.50 4.00 3.50 3.00 2.50
Phase velocity (km/sec)

FIGURE 4b.

FIGURE 5a.

FIGURE 5b.


NORSAR
ALPA
LASA
6'
8
7
9
9'
5
4
11
5
12
13
11
3
5
2
9
1
11
10
13
4
5
7
6
9
16
12

FIGURE 6.

Paper II

Persistent Primary Microseisms Observed During Northern and Southern Hemisphere Peak Storm Months

by
Robert K. Cessaro
Teledyne Geotech Alexandria Laboratories
314 Montgomery Street
Alexandria, VA 22314

Submitted to:
Geophysical Research Letters

Persistent Primary Microseisms Observed During Northern and Southern Hemisphere Peak Storm Months

ROBERT K. CESSARO

Teledyne Geotech Alexandria Laboratories, Alexandria, Virginia

For submission to Geophysical Research Letters

ABSTRACT

Sources of microseisms, routinely observed as coherent low-frequency noise between 10 and 200 mHz from seismic records made throughout the world, appear to be somewhat predictable. They have been observed to emanate preferentially from certain near-coastal regions in the northern hemisphere during the peak activity of pelagic storms with trajectories in the N. Atlantic and N. Pacific ocean basins. One question raised by that observation is whether there are other similar source locations. This paper addresses that question by reporting on results of analysis of microseisms recorded during the peak pelagic storm months for the southern hemisphere. It is probable that no microseisms were observed from the southern hemisphere in the earlier analysis, because it was performed on seismic array data recorded during northern hemisphere peak storm months. When data associated with the peak storm months for the southern hemisphere were analyzed, sources from southerly directions were consistently observed. It is therefore suggested that the existence of persistent primary microseism sources is not unique to the northern hemisphere and that there may be many other such sources on the planet awaiting discovery.

INTRODUCTION

Microseisms are commonly observed on seismic records as persistent and relatively coherent low-frequency noise between 10 and 200 mHz. Locating their source has been an important research objective since they were first observed in the 19th century. Over the years, many observations from recordings made by land- and ocean bottom-based seismo-acoustic systems have improved our understanding of these ubiquitous noise sources. Microseisms are characterized by long period waves that propagate into the continental interior as Rayleigh waves. Their association with meteorological storm systems in the ocean has been noted since the early part of this century (Wiechert,1904). They are generally identified as primary and secondary microseisms, exhibiting distinct spectral peaks at approximately 80 mHz and 150 mHz, respectively (Haubrich *et al.*, 1963). Primary microseisms typically exhibit dominant periods twice that of the related secondary microseisms (e.g., Oliver and Page, 1963).

Several mechanisms for the generation of primary and secondary microseisms have been put forward in recent work. The spectral peak of primary microseisms, observed on land between about 40 and 80 mHz, reflects the wavelengths of the dominant ocean waves and appears to form in shallow water by the forcing of a shoaling ocean bottom by incident ocean swells (*Oliver*, 1962; Haubrich *et al.*, 1963; Hasselmann, 1963). A study by Ostrovsky (1979) suggests that steep coasts would tend to favor the production of primary microseisms. Hasselmann (1963) showed that microseisms are generated by those spectral components of the random surface gravity wavefield that are well coupled to the local elastic media, either the ocean bottom or the continental platform. Several studies show that microseisms recorded on the ocean-bottom are similar to those recorded on the continent and are well correlated with known storm systems (e.g., Latham and Sutton, 1966; Latham and

Nowroozi, 1968). Analysis of ocean bottom records suggests that microseisms arise from non-linear storm wave interactions (Ostrovsky and Rykunov, 1982) and atmospheric pressure variations associated with storm passage (Webb and Cox, 1986).

Some recent studies of microseisms have sought to determine their directions of approach, phase velocity and source locations. Using wide angle triangulation from land-based arrays, Cessaro and Chan (1989) located two persistent near-shore sources of strong coherent primary microseisms during the peak storm months of the northern hemisphere. One source was located near the coast of Labrador and the other was near Queen Charlotte Island. That work was later corroborated and extended to secondary microseisms for a more extensive data sample (Cessaro, 1991; Cessaro, 1992). Again, these two primary microseism source locations were observed. Secondary microseism sources were also observed at these locations in addition to meandering oceanic locations more closely associated with the storm trajectories. The discovery that certain near-coastal locations may preferentially generate coherent microseisms in both bands has prompted research that seeks to model these locations realistically as a means of identifying the properties that would explain these observations (Yamamoto, personal communication).

In an effort to determine if there are other persistent source locations for primary microseisms, a larger set of low-frequency seismic data samples was extracted from LASA and ALPA array records and analyzed for the presence of coherent primary microseisms. These data represent a total time span of 88 days sampled during the months of October--December and May--August of 1970 through 1973. These months are typically associated with peak microseismic noise levels for northern and southern hemispheres respectively. The observations reported here are similar to those made in earlier work (Cessaro and Chan, 1989; Cessaro, 1992) but include one additional source location in the northern hemisphere

during the October-November time frame and another during June, as well as two persistent southern source azimuths during May and August. Wide angle triangulation was performed with data recorded in May and June for two source locations in the northern hemisphere. Primary microseisms arriving from the southern hemisphere, although persistent in approach azimuths found from analysis of the LASA array records, were not strong enough to be recorded by the ALPA array.

DATA DESCRIPTION

The low-frequency microseism signals are obtained from digitized recordings collected by the Montana Large Aperture Seismic Array (LASA) and the Alaskan Long Period Array (ALPA) for the times shown in Table 1. The data sample times were selected to span the season of peak storm activity in the northern and southern hemispheres while the two arrays were in operation. Historical records of southern hemisphere principal storm tracks during the study period are apparently not available.

Table 1 - Data sampled for this study.

Years	Arrays	
	LASA	ALPA
1970	17 Oct -- 3 Dec	
1971	1 -- 16 May	6 -- 13 May
1971	24 Aug -- 1 Sep	
1973	1 -- 12 May	1 -- 12 May
1973	3 -- 11 Jun	3 -- 11 Jun

The LASA array, operating from 1965 through 1978, included 21 three-component long-period seismometers. The ALPA array, operating from 1970 through 1982, was composed of 19 long-period triaxial seismometers. The arrays recorded digitally at 1-Hz sampling frequency. The frequency response of the long-period elements of the arrays is flat to velocity

from 25- to 200-second period (5-40 mHz). The location and pattern of these arrays are published elsewhere (*e.g.*, Figure 1 of Cessaro, 1992).

Continuous 4000-second data samples are excerpted for analysis on an interval of approximately 6-hours from the long-period array data archive stored at Teledyne Geotech Alexandria Laboratories. Signals are taken from vertical-component channels for LASA and the mathematically-rotated vertical component channels for ALPA. Signals are bandpass filtered using 4-pole Butterworth filters centered at 16-sec (0.06 Hz). No attempt is made to correct for instrument response (nominally 25 sec resonance peak), since it provides no advantage for FK analysis.

Some of the data samples are shifted by an hour or so from the regular 6-hour interval in order to avoid large earthquake phases exhibiting substantial power in the same pass band. The earthquake phases are confirmed on the ISC Bulletin reporting origin times, hypocenters and low-frequency earthquake phases (LQ and LR) and also serve to calibrate the accuracy of the microseism approach azimuths obtained from the FK analysis for similar azimuths. Over the the range of azimuths encountered for the microseisms, it appears that approach azimuths determined for the microseisms are reliable to within one degree of theoretical.

ANALYSIS

Frequency-wavenumber analysis

Frequency wavenumber (FK) analysis is performed on samples of low-frequency ambient noise recorded during the time periods shown in Table 1. The noise records are decomposed

into units of power by phase velocity and approach azimuth. The noise power consists of both coherent and incoherent components. The incoherent component, primarily from sources near the array, does not appear as separable power peaks in the FK analysis. The coherent component consists of microseisms from multiple sources and low-frequency earthquake phases.

Microseisms arriving as surface waves from pelagic storms are examined in phase velocity and direction of approach by using a sliding-window, broad-band FK technique (Capon, 1969) on 4000 sec bandpassed digitized array data samples. Although the term 'FK' is used here, the analysis is more accurately described as frequency-slowness analysis, because the FK power spectra are examined for a specific band-limited frequency plane. FK analysis is performed on sequential 128-second data segments in the 4000-sec data sample. Signal time windows are advanced by 100 seconds from previous windows, resulting in adjacent window overlaps of 28 seconds. Resulting estimates of approach azimuth and phase velocity are collected and examined for consistency and distribution. Multiple FK power peaks obtained from each 4000-sec data sample provide many approach azimuths that may contribute to the suite of potential microseismic source locations. The approach azimuths used are limited to those associated with phase velocity measurements between 3.0 and 4.0 km/sec conforming to observation that microseisms propagate primarily in the form of Rayleigh waves (*e.g.*, Cessaro and Chan, 1989). Time windows containing low-frequency phases from known earthquakes are excluded from this analysis to avoid unnecessary contamination.

Obtaining microseism source locations by triangulation

Where possible, a wide aperture triangulation is performed by combining estimates of approach azimuths obtained from overlapping FK analysis of ALPA and LASA array data. The

estimates of azimuth and velocity stability and associated errors are obtained from the distribution of approach azimuths, velocity and their corresponding FK power. In this way, each 4000-sec data sample provides multiple representative approach azimuths along with corresponding estimates of their reliability. Figure 1 shows an example of the distribution for primary microseism approach azimuths determined for the data sampled from the LASA arrays over the time period Oct. 17 through Dec. 3, 1970. A qualitative estimate of azimuth reliability is drawn from the half power azimuth limits. The intersection of the map projections of simultaneous azimuths and error estimates from their respective arrays provide bounding estimates of the microseism source location.

RESULTS AND DISCUSSION

The FK analysis employed in this study provides a measure of the well-coupled coherent fraction of the total storm-related microseismic noise field. Primary microseisms are observed to arise from deterministic spatially limited coastal sources that persist while there are ocean surface gravity waves of sufficient intensity incident at these locations.

Over the time period Oct 17 - Dec. 3, 1970 records for ALPA were not available, but the persistent approach azimuths and their similarity with earlier results argue for limited near-coastal source locations (Figure 2a). Wide angle triangulation using approach azimuths obtained by these methods was possible only for the primary microseism sources located in the northern hemisphere (Figure 2b, d, and e). The May 1971 data sampled from both arrays (Figure 2b) indicates two possible source locations; one near the Queen Charlotte Islands, as observed in earlier studies (Cessaro and Chan, 1989; Cessaro, 1992) and one to the south. The southern triangulation position is probably specious given the relatively low microseism power level at LASA and even lower at ALPA. It is significant that the microseism

source asssociated with a southwest approach azimuth as observed in the LASA data was persistent and exhibited twice the power of the source to the northwest. A similar result is obtained during May 1973 (Figure 2d) and is consistent with a single spatially limited source similar to those found in the northern hemisphere. Data sampled during August 1971 (Figure 2c) suggests two source locations, one that is likely to be near Queen Charlotte Islands and the other stronger microseism source generating waves that arrive from the west. Analysis of the August data sample was possible only with LASA data due to recording drop-outs and system noise in the ALPA data. The June 1973 (Figure 2e) triangulation position is similar to that cited in earlier work for the November 1973 time frame (Cessaro, 1992). It does, however, appear to be located in a more southerly position, perhaps reflecting a different dominant direction for the arriving southern hemisphere storm waves. Again, it is noted that primary microseisms have persistent near-shore locations not well correlated with their associated pelagic storm locations. Three primary microseism source locations are represented for Atlantic storms by these observations: two sources along the coast of Labrador during the the peak storm months of the northern hemisphere and one further south along the coasts of Nova Scotia and the Island of Newfoundland during the peak storm months of the southern hemisphere. Pacific storms correlate with a microseism source near the west coast of the Queen Charlotte Islands, BC, during the peak storm months of both the north and south Pacific.

The persistent appearance of just one north Pacific source location for primary microseisms during both the north and south Pacific storm seasons may be due to the relative openess of the Pacific. Ocean surface gravity waves generated in the south Pacific propagate more freely to the north than do similar waves in the south Atlantic. Ocean waves from storms in the south Atlantic are more strongly subject to refraction and reflection from the intervening coasts as they propagate to the primary microseism source locations cited

here. The distinction between the Labrador coast as the source of microseisms associated with north Atlantic storms and the source near the Gulf of St. Lawrence for south Atlantic storms may simply reflect a difference in the associated dominant surface gravity wave directions.

CONCLUSION

Although pelagic storms provide the source of microseismic wave energy, it appears that the dominant production of microseisms is controlled by an interplay between the pelagic storm wave power distribution, the direction of storm wave propagation, and near-shore elastic properties. The method described here is sensitive to only the well-coupled spectral components of the total pelagic storm-related random noise field.

There appear to be at least four specific near-shore regions in the northern hemisphere that generate microseisms strong enough to be observed as persistent FK power peaks in the primary-microseism band by the methods described here. The activity at some of these locations appears to be influenced by storm wave approach directions. Three primary microseism source locations are represented for Atlantic storms by these observations. Two sources near the coast of Labrador are associated with N. Atlantic storms (*cf.* Cessaro, 1992). The remaining source observed further south along the coasts of Nova Scotia and the Island of Newfoundland is associated with storms of the S. Atlantic. The coastal N. Pacific location near the west coast of the Queen Charlotte Islands, BC, appears to be associated with storm activity in both north and south Pacific. Two other Pacific ocean sources appearing in the records made during peak southern hemisphere storm months (May 1971, 1973 and August 1973) are not observed from the records made during the peak storm months of the northern hemisphere. Although it is likely that their associated microseism sources on those

azimuths are located in the southern hemisphere, triangulation was not possible because the microseisms were strong enough to be recorded only by the LASA array during the study period. More research may permit triangulation for these azimuths during periods of greater microseism amplitudes. There may well be other sources of primary microseisms that will emerge from further studies.

REFERENCES

Capon, J. (1969). High resolution frequency-wavenumber spectrum analysis, *Proc. IEEE*, **57**, 1408-1418.

Capon, J. (1970). Analysis of Rayleigh-wave multipath propagation at LASA, *Bull. Seism. Soc. Am.*, **60**, 1701-1731.

Cessaro, R. K. (1992). Sources of primary and secondary microseisms, submitted to *Bull. Seismol. Soc.*.

Cessaro, R. K. (1991). Seismic Array Study of Primary and Secondary Microseisms. Abstract, *EOS, Trans. Am. Geophs. Un.*, **72**, 302-303.

Cessaro, R. K. and W. W. Chan (1989). Wide-angle triangulation array study of simultaneous primary microseism sources. *J. Geophys. Res.*, **94**:15,555-15,563.

Hasselmann, K. A. (1963). A statistical analysis of the generation of microseisms, *Rev. Geophys.*, **1**, 177-210.

Haubrich, R. A., Munk, W. H. and F. E. Snodgrass (1963). Comparative spectra of microseisms and swell, *Bull. Seism. Soc. Am.*, **53**, 27-37.

Iyer, H. M. (1958). A study of direction of arrival of microseisms at Kew Observatory, *Geophys. J.*, **1**, 32-43.

Latham, G. V. and A. A. Nowroozi (1968). Waves, weather, and ocean bottom microseisms, *J. Geophys. Res.*, **73**, 3945-3956.

Latham, G. V. and G. H. Sutton (1966). Seismic measurements on the ocean floor, 1. Bermuda Area, *J. Geophys. Res.*, **71**, 2545-2573.

Oliver, J. (1962). A worldwide storm of microseisms with periods of about 27 seconds, *Bull. Seism. Soc. Am.*, **52**, 507-517.

Oliver, J. and R. Page (1963). Concurrent storms of long and ultra-long period microseisms, *Bull. Seism. Soc. Am.*, **53**, 15-26.

Ostrovsky, A. A., 1979. On some characteristics of microseismic sources, *Izvestiya, Earth Physics*, **15**, 825-828.

Ostrovsky, A. A. and L. N. Rykunov (1982). Experimental study of ocean bottom seismic noise during passage of a cyclone, *Oceanology*, **22**, 720-722.

Webb, S. C., and C. S. Cox, 1986. Observations and modeling of seafloor microseisms, *J. Geophys. Res.*, **91**, 7343-7358.

Wiechert, E. (1904). *Verhandlungen der Zweiten Internationalen Seismologischen Konferenz. Gerl. Beitr. Geophys.*, Erganzungsbd. **2**, 41-43.

FIGURES

Figure 1. An example of the stacked FK power distribution for primary microseisms recorded on the LASA long period array for the sample period Oct. 15 - Nov. 30, 1970.

Figure 2. These maps show persistent primary microseism source azimuths and error estimates drawn from half power bounds of power vs. azimuth as shown in Figure 1.

(a) Maximum FK power in the primary microseism band appears in the same location as observed in earlier work. One additional location (3dB down from maximum) appears further north along the Labrador coast. West coast source near Queen Charlotte Island is identical to earlier results. Records were not available for 1970 ALPA sample period.

(b) The May 1971 sample indicates two strong source azimuths in the LASA records an one in the ALPA records. It is probable that only the northernmost triangulation location is accurate: it is unlikely that two source locations would have the same azimuth as 'seen' from ALPA.

(c) The August sample was only possible with LASA data due to problems with the ALPA data. Two source azimuths appear; one probably associated with the Queen Charlotte Islands location and the stronger source arriving from the west.

(d) The May 1973 sample exhibits results similar to those obtained for May 1973: again suggesting a source in the southern hemisphere.

(e) The June 1973 sample indicates a triangulation location similar to that found during the activity of north Atlantic storms, but located further south near the Gulf of St. Lawrence.

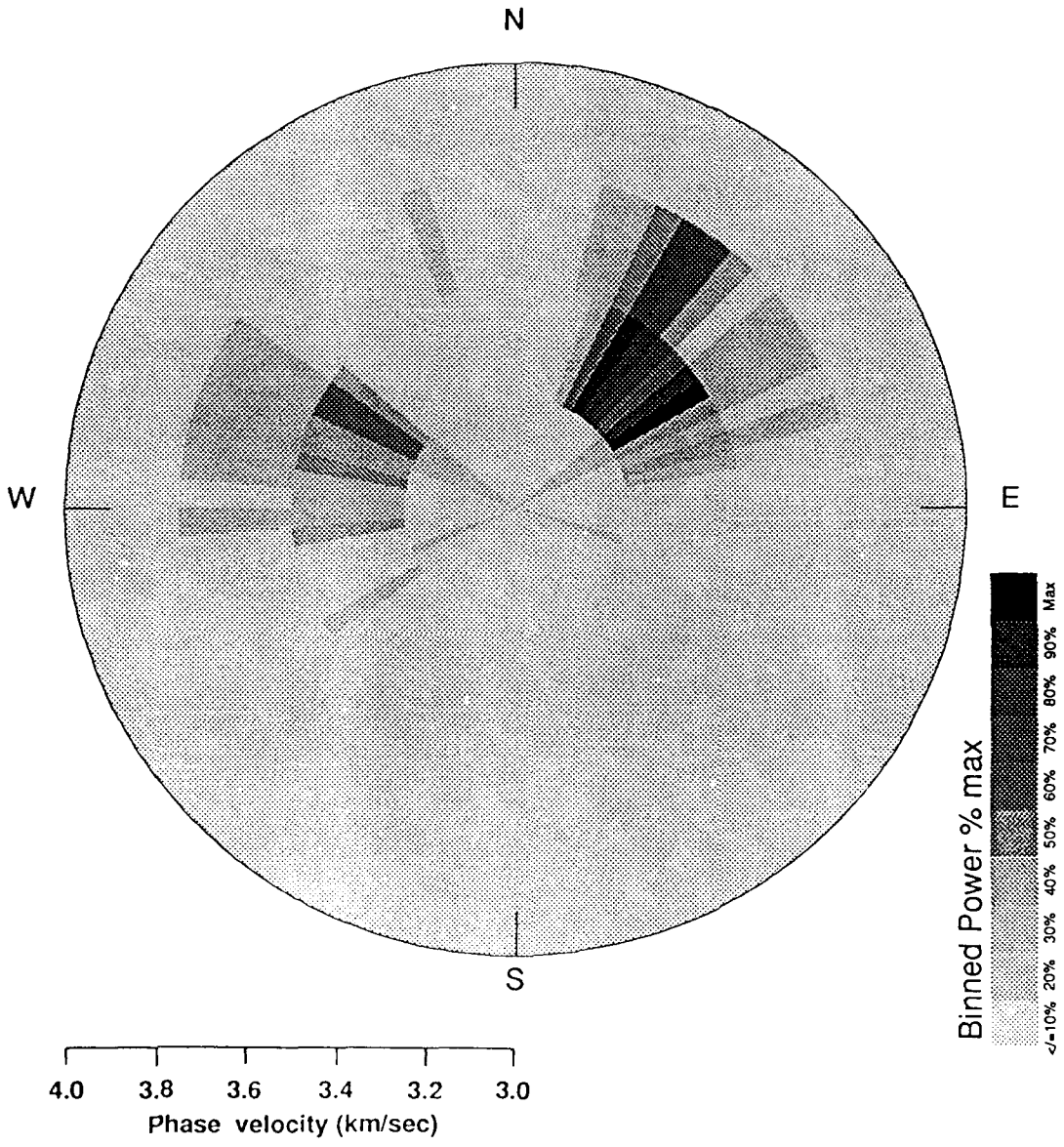
N
W
E
S
4.0
3.8
3.6
3.4
3.2
3.0
Phase velocity (km/sec)
Binned Power % max
</=10%
20%
30%
40%
50%
60%
70%
80%
90%
Max

FIGURE 1.

2a.

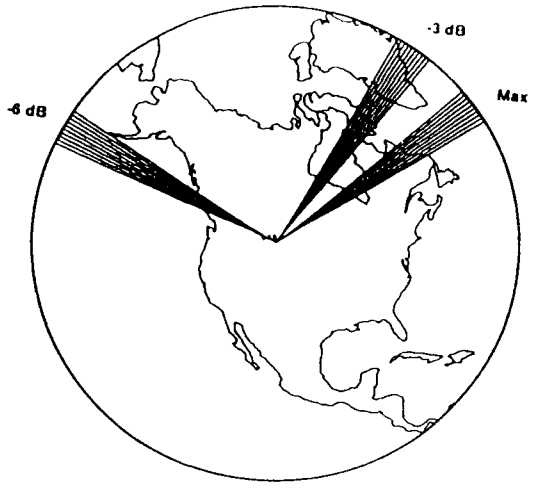

2b.

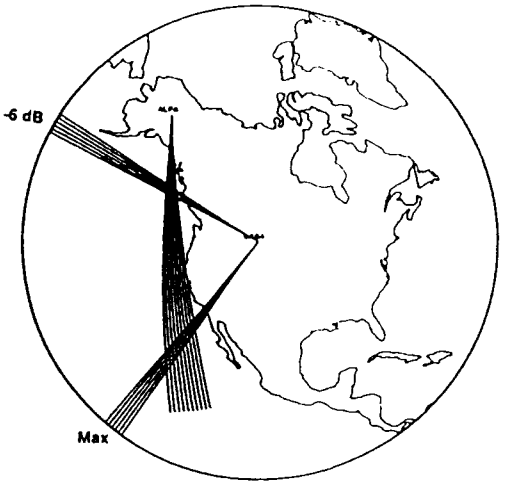

2c.

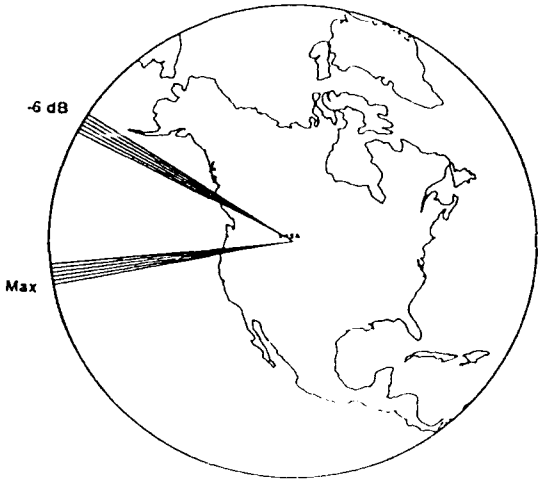

2d.

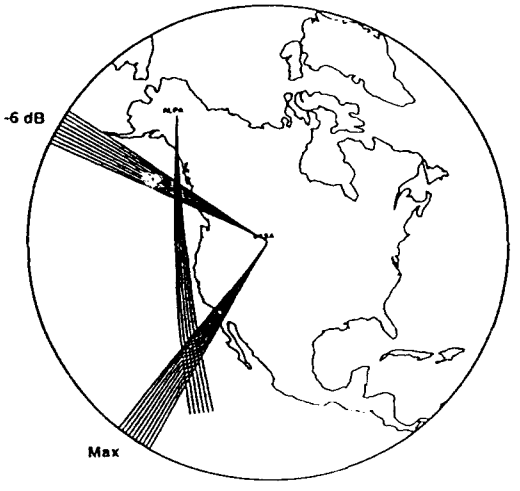

2e.